Musculoskeletal Morphology and Strength of the Foot and Ankle in Pediatric Charcot-Marie-Tooth Disease

Melissa R. Requist[1], Curran Reddy[1], Andrew C. Peterson[1], Erika Muhlrad[1], Megan Mills[1], Theresa Hennessey[1,2], Kristen Carroll[1,2], Russell J. Butterfield[1,2], Amy L. Lenz[1]
[1]University of Utah, Salt Lake City, UT, [2]Shriners Hospital for Children, Salt Lake City, UT
melissa.requist@hsc.utah.edu

Disclosures: Melissa R. Requist (N), Curran Reddy (N), Andrew C. Peterson (N), Erika Muhlrad (N), Megan Mills (N), Theresa Hennessy (N), Kristen Carroll (N), Russell J. Butterfield (3B; Sarepta, Scholar Rock, Precision Bio, Novartis. 5; Ionis Pharmaceuticals),, Amy L. Lenz (N)

INTRODUCTION: Charcot-Marie-Tooth disease (CMT) is an inherited progressive peripheral neuropathy that typically presents in childhood or adolescence with muscle weakness, sensory deficit, or cavovarus foot deformity [1,2]. This characteristic cavovarus deformity present in adolescents with CMT is believed to develop out of the typical flat foot of childhood due to imbalances in muscle strength in the limb [2-4]. In the adult population, individuals with CMT demonstrate differences in osseous morphology and bony alignment of the foot consisting primarily of varus hindfoot, high arch, rotation and flattening of the talus, and plantar-valgus bending of the metatarsals [5-7]. These studies have primarily used weight-bearing computed tomography (WBCT) to assess skeletal morphology under normal loading. Magnetic resonance imaging (MRI) has shown increased fat fraction in lower limb muscles in CMT but has not been used to relate muscle morphology to strength [8]. Statistical shape modeling (SSM) is a computational tool able to describe differences in three-dimensional geometry of anatomic structures and has been used to describe bony morphology in adult CMT, muscle morphology in cerebral palsy, and combined bone and tibialis posterior structure in progressive collapsing foot deformity; however, combined models of musculoskeletal anatomy of the leg have not been previously described, nor have the morphologic characteristics of the foot and ankle in children with CMT [6,7,9,10]. This study aims to utilize WBCT and MRI to generate an SSM of major musculoskeletal structures of the leg and to correlate morphology variation with dorsiflexion and plantarflexion strength.

METHODS: Following informed consent, imaging of the foot and ankle, consisting of WBCT and MRI was acquired from 5 children with CMT (average age 12.6, 1 F) and 4 controls (average age 12.3, 1 F). Demographics between groups were compared with a t-test and chi square test. WBCT images were reconstructed with a 0.37 mm^3 voxel size from cone beam CT with participants standing in a neutral position. MR images were acquired using a 3 Tesla scanner with a T1-weighted DIXON sequence at a $1mm^3$ uniform voxel size for visualization of muscles and utilized a foot plate to maintain a neutral position of the ankle [11,12]. Average plantarflexion and dorsiflexion strength in the CMT cohort was measured bilaterally using a handheld dynamometer with three trials of each measure [4]. Bones from the tibia through metatarsals were segmented from WBCT semi-automatically (Bonelogic, DISIOR) followed by manual verification and cleanup (Mimics, Materialise). Muscle bellies of the soleus, lateral and medial gastrocnemius, and tibialis anterior and posterior were semi-automatically segmented from in-phase MRI scans (Mimics, Materialise). Bony segmentations were coregistered with MR models through manual landmark-based registration focused on the distal tibia. All three-dimensional parts were consistently smoothed and decimated then aligned with iterative closest point alignment of the combined bone and muscle structure. A 19-structure multi-domain SSM was generated with a single-domain optimization for multi-domain modelling pipeline [7]. The SSM was analyzed with principal component analysis (PCA) followed by parallel analysis, yielding modes of variation representing more than a proportion of population variance. Differences between groups in PCA component scores along each mode were analyzed with a Wilcoxon rank sum test. Relationship between shape scores and strength was tested with a linear regression and difference in strength between limbs above and below the mean shape score of the PCA mode was tested with a one-sided Wilcoxon rank sum test. Morphologic differences were further assessed with a Hotelling's T^2 test to compare particle distance differences from the mean shape between groups. This test was conducted for each muscle or bone in its local coordinate system to assess differences in shape and in the global coordinate system to assess differences in alignment [7]. Statistical tests used significance $\alpha = 0.05$.

RESULTS: There were no differences in age or sex distribution between CMT and control groups. The first and second PCA modes of the SSM demonstrated variation in size and positioning that were not different between groups. However, the third mode of variation (Figure 1A) showed variation in the medial and lateral gastrocnemius morphology that, while not statistically significant due to the small sample size, had a trend towards a more cavovarus foot with thicker medial gastrocnemius head and medial shift of the both gastrocnemius heads relative to the soleus in the CMT group. This variation in muscle morphology co-occurred with a more varus position of the calcaneus. Results from the Hotelling's T^2 test support these findings, with differences in alignment between CMT and control groups primarily in the posterior calcaneus and differences in shape present throughout the medial gastrocnemius and head of the lateral gastrocnemius. There was no significant correlation between plantarflexion strength and shape score and a weak correlation between dorsiflexion strength and shape score (R^2 = 0.33) (Figure 2). For both dorsiflexion and plantarflexion strength, the limbs with a positive shape score, indicating a more cavovarus foot, had lower strength than the limbs with a negative shape score ($p = 0.048$).

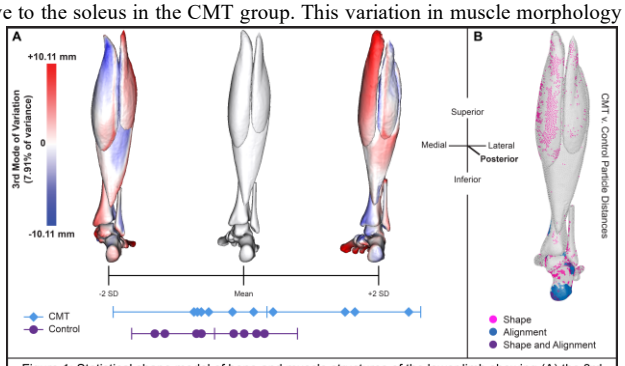

Figure 1: Statistical shape model of bone and muscle structures of the lower limb showing (A) the 3rd PCA mode of variation demonstrating a difference in cavovarus foot position and medial versus lateral proximal gastrocnemius thickness with red and blue representing positive and negative distance to the mean shape and distributions of the shape scores of CMT and control groups shown in blue and purple and (B) Hotelling's T^2 test results with highlighted particles representing a significant difference in particle distance between CMT and control groups where pink indicates a difference due to shape variation, blue indicates a difference due to alignment, and purple represents a difference in both shape and alignment

DISCUSSION: These data represent a novel model of musculoskeletal morphology in adolescents with CMT. While this preliminary analysis is limited by sample size, it suggests that thickening the cavovarus position of the foot in CMT may have associated hypertrophy of the medial gastrocnemius head. Further, this study provides some evidence that the overall musculoskeletal anatomy of the leg may be related to dorsiflexion and plantarflexion strength. In both cases, the direction of causation is unknown and may be confounded by age since both the cavovarus deformity and muscle strength are impacted by disease progression.

SIGNIFICANCE/CLINICAL RELEVANCE: This image-based model of musculoskeletal morphology allows for detailed analysis of the relationships between bone and muscle morphology, muscle strength, and function in children with CMT and suggests a difference in proximal medial gastrocnemius head morphology that may be related to cavovarus foot deformity and decreased strength in this population.

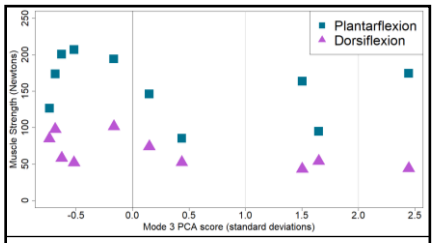

Figure 2: Scatterplot of plantarflexion and dorsiflexion strength compared to PCA mode 3 shape score. More positive shape scores represent a more varus hindfoot with thicker medial gastrocnemius

ACKNOWLEDGEMENTS: This work was supported by the Utah MR Research Center team and grant S10OD026788. Funding was provided by University of Utah Pediatric Orthopaedics Foundation Grant.

REFERENCES: [1] Corrado B. Medicine (Baltimore). 2016. 95(17): e3278. [2] Rambelli C. Fron Hum Neurosci. 2022. 16: 914340. [3] Cornett KMD. JAMA Neurol. 2017. 37(6): 645-51. [4] Burns J. Ann Neurol. 2012. 71(5): 642-52. [5] Michalski M. Foot Ankle Int. 2022. 43(4): 576-81. [6] Requist MR. JBMR Plus. 2025. 9(6): ziaf058. [7] Requist MR. Foot Ankle Int. 2025. (accepted). [8] Evans MRB. Ann Clin Transl Neurol. 2025. 12(4): 756-67. [9] Bin Ghouth SG. Sci Rep. 2022. 12(1): 7711. [10] Miyamoto T. JBJS Open Acc. 2025. (rest) [11] Engelke K. J Orthop Translat. 2023. 42: 57-72.